Inorganic Chemistry

Article

pubs.acs.org/IC

Pentanuclear Cyanide-Bridged Complexes Based on Highly Anisotropic Co^{II} Seven-Coordinate Building Blocks: Synthesis, Structure, and Magnetic Behavior

Luke J. Batchelor,*[,†] Marco Sangalli,[†] Régis Guillot,[†] Nathalie Guihéry,[‡] Remi Maurice,[‡,∥] Floriana Tuna,[§] and Talal Mallah*[,†]

[†]Institut de Chimie Moléculaire et des Matériaux d'Orsay, CNRS, Université Paris-Sud 11, 91405 Orsay, France

[‡]Laboratoire de Chimie et Physique Quantiques, CNRS, Université Paul Sabatier, 118 route de Narbonne, 31062 Toulouse Cedex 09, France

[§]School of Chemistry, The University of Manchester, Oxford Road, Manchester M13 9PL, United Kingdom

[∥]Departament de Química Física i Inorganica, Universitat Rovira i Virgili, Marcel.lí Domingo s/n, 43007 Tarragona, Spain

Supporting Information

ABSTRACT: Pentagonal-bipyramidal complexes [Co(DABPH)X(H_2O)]X [X = NO_3 (**1**), Br (**2**), I (**3**)] were synthesized, and their magnetic behavior was investigated. Simulation of the magnetization versus temperature data revealed the complexes to be highly anisotropic ($D \approx +30$ cm^{-1}) and the magnitude of the anisotropy to be independent of the nature of the axial ligands. The reaction of **1** with $K_3[M(CN)_6]$ (M = Cr, Fe) produces the pentametallic clusters $[\{Co(DABPH)\}_3\{M(CN)_6\}_2(H_2O)_2]$ [M = Cr (**4**), Fe (**5**)]. Both clusters consist of three {Co(DABPH)} moieties separated by two $\{M(CN)_6\}$ fragments. In **4**, the central and terminal Co^{II} ions are bound to cyanide groups cis to one another on the bridging $\{Cr(CN)_6\}$, whereas in **5**, the connections are via trans cyanide ligands, resulting in the zigzag and linear structures observed, respectively. Magnetic investigation revealed ferromagnetic intramolecular interactions; however, the ground states were poorly isolated because of the large positive local anisotropies of the Co^{II} ions. The effects of the local anisotropies appeared to dominate the behavior in **5**, where the magnetic axes of the Co^{II} ions were approximately colinear, compared to **4**, where they were closer to orthogonal.

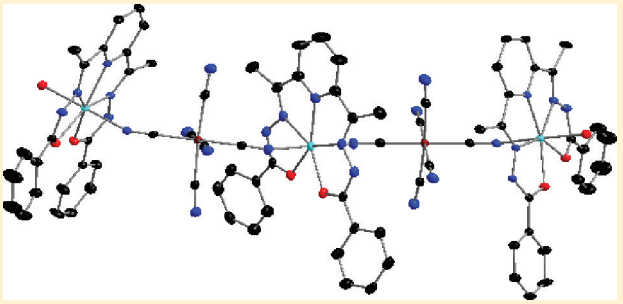

INTRODUCTION

Polynuclear complexes of first-row transition-metal ions have the potential to behave as single molecule magnets (SMMs),[1] eventually capable of storing[2] and processing[3] information at the molecular level. The SMM behavior stems from a high-spin ground state and a strong Ising-type anisotropy, which leads to a barrier for the reorientation of the magnetization and subsequent blocking below a given temperature. Access to clusters with high-spin ground states is increasingly available with our understanding of the structural motifs that promote ferromagnetic exchange between metal centers,[4,5] and the development of clusters with large axial anisotropies, which may lead to Ising-type anisotropy, is arguably the harder challenge in the search for new SMMs. One of the major sources of anisotropy in polymetallic clusters is single-ion anisotropy.[6] Large axial anisotropy is the result of the simultaneous effects of spin−orbit coupling (SOC) and axial symmetry. Thus, the use of axial building blocks to construct high-nuclearity clusters is a possible route to large magnetic anisotropy in molecular complexes.

First-order SOC is present for Co^{II} in O_h symmetry. However, the degeneracy of the $^4T_{1g}$ ground state is lifted via minor distortions, resulting in most cases in a $^4A_{2g}$ ground state and a ^4E_g excited state. Provided the separation between $^4A_{2g}$ and ^4E_g is large enough, only the two lowest-energy Kramers doublets ($M = \pm^1/_2$) are populated, the separation between which is $2D$.[7] For six-coordinate Co^{II}, D can be very large, up to +83 cm^{-1},[8] and although always positive, the correct alignment of the axial zero-field-splitting (ZFS) tensor of each metal center may result in molecular Ising-type anisotropies. SMM behavior in a Co^{II} cluster was first reported for $[Co_4(hmp)_4(MeOH)_4Cl_4]$ in 2002,[9] and since then, energy barriers for relaxation as high as 84 K for octametallic phosphonate-bridged clusters[10] or 96 K for a Co^{II} dimer in which bridging carbene ligands introduce additional spin upon radiation have been reported.[11]

The ground state of seven-coordinate Co(II) complexes is not orbitally degenerate and well separated from other excited states. However, the axiality of the pentagonal-bipyramidal

Received: July 20, 2011
Published: November 3, 2011

Table 1. Details of the Crystallographic Analysis of 2, 4, and 5

	2	4	5
chemical formula	$C_{23}H_{25}N_5CoI_2O_4$	$C_{89}H_{57}N_{27}Co_3Cr_2O_{36}$	$C_{81}H_{103}N_{27}Co_3Fe_2O_{26}$
mol wt	748.21	2361.41	2159.39
crystal dimens/mm	0.20 × 0.20 × 0.03	0.33 × 0.08 × 0.01	0.20 × 0.17 × 0.03
cryst syst	monoclinic	monoclinic	monoclinic
space group	$P2_1/n$	$C2/c$	$C2/c$
a/Å	8.0749(5)	36.133(5)	33.312(2)
b/Å	14.2955(8)	32.248(5)	16.7668(9)
c/Å	22.8291(14)	10.7698(12)	17.1653(10)
α/deg	90.00	90.00	90.00
β/deg	99.069(2)	101.268(3)	95.861(2)
γ/deg	90.00	90.00	90.00
U/Å^3	2602.3(3)	12307(3)	9537.5(10)
Z	4	4	4
ρ_{calcd}	1.910	1.274	1.504
T/K	100(1)	100(1)	100(1)
$2\theta_{max}$/deg	34.34	23.25	31.51
data collected	12 364	66 150	15 835
unique reflns	9146	8720	11 110
no. of param	318	712	631
final R1, wR2 [$I > 2\sigma(I)$] (all data)	0.0318, 0.0622 (0.0547, 0.0668)	0.0893, 0.2378 (0.1921, 0.3088)	0.0470, 0.1167 (0.0805, 0.1321)

geometry may lead to large anisotropy. D = +25 cm^{-1} was reported for an axially compressed Co^{II} complex formed using a heptadentate lariat ether *N*,*N*′-bis(2-aminobenzyl)-1,10-diaza-15-crown-5.[12] To date, no quantitative rationalization has been undertaken and there have been virtually no attempts to incorporate such complexes as building blocks for larger clusters. The primary routes toward seven-coordinate Co^{II} complexes are via the use of heptadentate ligands, either cyclic (funtionalized crown ethers)[13] or acyclic (tren derivatives).[14] However, these are poor candidates for large cluster development because of the absence of labile ligands that can be substituted to form polymetallic complexes. Complexes possessing pentadentate equatorial ligands and labile axial ones may be accessed using crown ethers[15] or Schiff base type compounds,[16] usually synthesized initially from diacetylpyridine (with the possibility of further functionalization).

Examples of seven-coordinate Co^{II} incorporated into clusters include the tetrametallic planar, linear array reported by Aromi et al., consisting of a pair of seven-coordinate Co^{II} ions, each also bound to a six-coordinate Co^{II} with linear tripyridyl/bis(β-diketone) ligands; however, antiferromagnetic exchange via the bridging O atoms results in a S = 0 ground state for the cluster,[17] as well as other bimetallic species for which magnetic data are not reported.[18] There is also one example of a three-dimensional helical metalloframework consisting of [Cr(CN)$_6$]$^{3-}$ units and seven-coordinate Co^{II} that exhibits long-range ferromagnetic order below 12 K.[19] Ferromagnetic exchange between Co^{II} centers is promoted by bridging [Cr(CN)$_6$]$^{3-}$ because the unpaired electron density is in orthogonal orbitals on Cr and Co, respectively, thus interacting with orthogonal cyanide-based orbitals and resulting in ferromagnetic exchange.[20] This is the case for [Co(tmphen)$_2$]$_3$[Cr(CN)$_6$]$_2$, reported by Dunbar et al., displaying a significant but unmodeled ferromagnetic exchange between the Co^{II} and Cr^{III} moieties,[21] and we will apply this principle to systems including seven-coordinate Co^{II}.

Herein we report the magnetic properties of the previously reported seven-coordinate Co^{II} complex [Co(DABPH)(H$_2$O)(NO$_3$)](NO$_3$) [**1**; DABPH = 2,6-diacetylpyridinebis(benzoic acid hydrazone)][22] and the synthesis and magnetic properties of similar complexes with different axial ligands. The synthesis of polymetallic assemblies from the reaction of the seven-coordinate Co^{II} complex with metallocyanides is also reported, with an accompanying magnetic investigation.

EXPERIMENTAL SECTION

Synthesis. Chemicals were purchased from Aldrich and used without further purification. DABPH and [Co(DABPH)(H$_2$O)(NO$_3$)](NO$_3$) (**1**) were synthesized according to literature procedures.[22] All solvents were from BDH and were used as received. All manipulations were conducted under standard benchtop conditions.

*Synthesis of [Co(DABPH)I(H$_2$O)]I·H$_2$O (**2**).* DABPH (0.150 g, 0.375 mmol) was suspended in H$_2$O (20 mL) and the temperature raised to 55 °C. CoI$_2$ (117 mg, 0.375 mmol) dissolved in EtOH (35 mL) was added dropwise with stirring, forming a pale-orange solution, which was stirred overnight at room temperature. This was then filtered and left to slowly evaporate, yielding red crystals after 4 days (0.085 g, 32%). Elem anal. Found (calcd for $CoC_{23}H_{25}N_5O_4I_2$): C, 36.72 (36.92); H, 3.31 (3.36); N, 9.31 (9.36). ESI$^+$-MS (MeOH): m/z 457.09 ([Co(DABPH)]{H$^+$})$^+$, 585.01 ([Co(DABPH)I]$^+$). IR (KBr, ν/cm^{-1}): 3461 (m), 3406 (m), 3324 (w), 3287 (w), 3178 (w), 3068 (m), 2918 (w), 1984 (w), 1642 (m), 1622 (s), 1577 (m), 1513 (s), 1481 (s), 1454 (m), 1426 (m), 1376 (m), 1310 (m), 1287 (s), 1178 (s), 1153 (m), 1128 (m), 1097 (w), 1074 (m), 1015 (w), 999 (w), 899 (w), 810 (m), 792 (w), 739 (w), 711 (s), 669 (m), 575 (w), 518 (w), 504 (w), 471 (m), 421 (m).

*Synthesis of [Co(DABPH)Br(H$_2$O)]Br·H$_2$O (**3**).* A reaction similar to that for **2** but with replacement of CoI$_2$ with CoBr$_2$·H$_2$O (0;088 g, 0.375 mmol) yielded brown crystals of **3** in comparable yield (0.100 g, 41%). Elem anal. Found (calcd for $CoC_{23}H_{25}N_5O_4Br_2$): C, 42.17 (42.12); H, 3.79 (3.85); N, 10.64 (10.70). ESI$^+$-MS (MeOH): m/z 457.09 ([Co(DABPH)]{H$^+$})$^+$. IR (KBr, ν/cm^{-1}): 3453 (m), 3396 (m), 3306 (m), 3195 (w), 3063 (m), 2979 (w), 2897 (m), 2798 (w), 1625 (s), 1578 (m), 1518 (s), 1484 (m), 1455 (m), 1429 (m), 1377 (w), 1313 (m), 1295 (s), 1279, (s), 1178 (s), 1153 (m), 1129 (m), 1097 (w), 1075 (m), 1017 (w), 1000 (w), 899 (w), 812 (m), 794 (w), 743 (w), 713 (s), 672 (m), 560 (w), 518 (w), 520 (w), 466 (m), 427 (m).

*Synthesis of [{Co(DABPH)}$_3${Cr(CN)$_6$}$_2$(H$_2$O)$_2$]·15H$_2$O (**4**).* K$_3$[Cr(CN)$_6$] (0.022 g, 0.067 mmol) dissolved in H$_2$O (15 mL) was added dropwise to a hot, stirred solution of **1** (0.040 g, 0.067 mmol) in

dx.doi.org/10.1021/ic201534e | Inorg. Chem. 2011, 50, 12045–12052

MeOH/H_2O (4:1, 75 mL). The clear yellow solution was stirred for 1 h at room temperature and then left to slowly evaporate. Yellow needle-shaped crystals of **4** (0.020 g, 48%) formed after 1 week. Elem anal. Found (calcd for $Co_3Cr_2C_{81}H_{97}N_{27}O_{23}$): C, 46.27 (46.36); H, 4.16 (4.66); N, 17.77 (17.55). IR (KBr, ν/cm^{-1}): 3375 (s), 2127 (w), 1624 (s), 1578 (m), 1527 (s), 1489 (m), 1440 (m), 1379 (m), 1293 (s), 1180 (m), 1135 (w), 1079 (w), 1020 (w), 1002 (w), 901 (w), 811 (m), 714 (m), 455 (m).

*Synthesis of [{Co(DABPH)}$_3${Fe(CN)$_6$}$_2$(H$_2$O)$_2$]·16H$_2$O (**5**).* $K_3[Fe(CN)_6]$ (0.029 g, 0.088 mmol) dissolved in H_2O (10 mL) was added dropwise to a hot, stirred solution of **1** (0.080 g, 0.133 mmol) in MeOH (20 mL). The mixture was stirred at 55 °C for 20 min, during which time **5** precipitated as a brown powder (0.040 g, 42%). It was isolated by filtration, washed with H_2O (5 mL) and MeOH (10 mL), and dried in air. The mother liquors were left to slowly evaporate, yielding X-ray-quality block-shaped crystals after 1 month. Elem anal. Found (calcd for $Co_3Fe_2C_{81}H_{99}N_{27}O_{24}$): C, 45.76 (45.79); H, 4.66 (4.70); N, 17.90 (17.81). IR (KBr, ν/cm^{-1}): 3400 (s), 2138 (m), 2114 (m), 1626 (s), 1578 (m), 1532 (m), 1489 (m), 1441 (m), 1379 (w), 1294 (s), 1180 (m), 1135 (w), 1079 (w), 1020 (w), 1002 (w), 901 (w), 810 (w), 715 (m), 692 (m), 567 (w), 526 (w).

Physical Measurements. IR data were measured on KBr pellets using a PerkinElmer FTIR spectrometer. Variable-temperature (300−2 K) magnetic data were measured on powdered samples of **1**−**5** in an eicosane matrix in 1.0 and 0.1 T fields using a Quantum Design MPMS5 SQUID magnetometer. The data were corrected for the diamagnetic contribution of the sample holder and eicosane, and the diamagnetism of the sample was estimated according to Pascal's constants. Low-temperature (2−6 K) variable-field (0−5.5 T) measurements were carried out in the same manner. Modeling of the magnetic susceptibility and magnetization data was performed by matrix diagonalization methods using *MAGPACK* software.[23]

X-ray Diffraction. Single-crystal X-ray diffraction data were measured on a Bruker APEX II CCD diffractometer. The diffraction intensities were collected with graphite-monochromatized Mo Kα radiation. The temperature of the crystal was maintained at the selected value (100 K) by means of a 700 series Cryostream cooling device to within an accuracy of ±1 K. Intensity data were corrected for Lorenz−polarization and absorption factors. Structure solution and refinement were performed using *SHELXS97* and *SHELXL97*.[24] The structures were refined by direct methods. Refinement of F^2 was against all reflections with anisotropic displacement parameters for all non-H atoms.

RESULTS

1 (Figure 1) was synthesized according to literature procedures and was characterized by mass spectrometry (MS), elemental analysis, and IR spectroscopy, and a unit cell was collected to ensure that the structure was identical with that previously reported.[22]

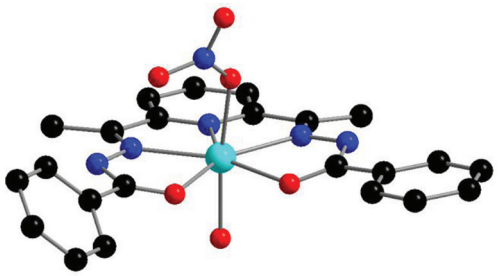

Figure 1. Previously reported structure of the cation in **1**. H atoms and counterions are omitted for clarity. Color code: Co, cyan; C, black; N, blue; O, red.

1 crystallizes in the monoclinic $P2_1/n$ space group, and the structure was fully described previously. The neutral DABPH ligand five-coordinates the Co^{II} ion around the equatorial plane, leaving the axial positions free for coordination by one water molecule and one nitrate ligand, thus completing the pentagonal-bipyramidal coordination sphere, with charge balance provided by the nitrate counterion.

The iodide and bromide analogues of **1** may be synthesized by the same procedure, upon replacement of $Co(NO_3)_2$ by CoI_2 or $CoBr_2$. The products were characterized by MS, elemental analysis, and IR spectroscopy, and a crystal structure of **2** was obtained (Figure 2).

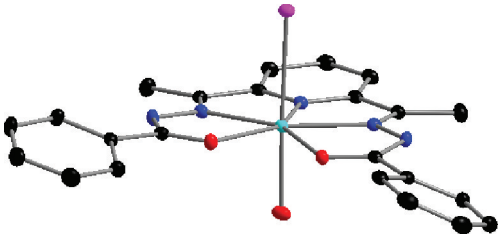

Figure 2. Structure of the cation in **2**. H atoms, counterions, and solvent molecules are omitted for clarity. Color code: Co, cyan; C, black; N, blue; O, red; I, purple. Thermal ellipsoids are shown at the 50% probability level.

2 crystallizes in the monoclinic $P2_1/c$ space group and consists of a pentagonal-bipyramidal cation, in which Co^{II} is ligated around the equatorial plane by a pentadentate DABPH ligand, with one iodide and one water molecule occupying the axial positions (at distances of 2.793 and 2.097 Å from the Co^{II} ion). Charge balance is provided by an iodide counterion, and there is one molecule of water in the crystal lattice. Globally, the structure is similar to that of **1**; however, the equatorial coordination is closer to pentagonal in **2** [ligand bite angles from 70.78° (for $N_{pyridyl}$−Co−N) to 74.73° (for O−Co−O), compared to 69.54−78.67° for the equivalent angles in **1**], and the terminal phenyl groups lie closer to the equatorial plane (torsion angles of 16.11 and 24.07° compared to 9.89 and 34.27°), which is likely due to the difference in packing due to the change in the counterion; there are fewer π-stacking and hydrogen-bonding interactions than in **1**, which has a significant hydrogen-bonding network via both the coordinated and counterionic nitrate ions and the lattice solvent water molecules.

The room temperature reaction of **1** with 1 equiv of $K_3[Cr(CN)_6]$ in MeOH/H_2O yields crystalline **4** (Figure 3) upon the slow evaporation of the reaction mixture.

4 crystallizes in the monoclinic $C2/c$ space group and consists of a neutral, pentametallic cluster containing three $\{Co(DABPH)\}^{2+}$ units bridged to one another via two $\{Cr(CN)_6\}^{3-}$ moieties in a zigzag fashion. The central seven-coordinate Co^{II} is coordinated equatorially by a DABPH ligand, slightly more symmetrically than that for monometallic complex **1** (ligand bite angles ranging from 70.47 to 77.33°, compared to 69.54−78.67°). The axial positions are ligated by the cyano N atoms of two crystallographically equivalent $\{Cr(CN)_6\}$ units (a Co−N bond length of 2.068 Å, slightly shorter than that reported for six-coordinate Co−NC bonds[21,25]); the cyanide bridge is far from linear with respect to the two metals (a Co−N−C angle of 154.58°). The geometry around the Cr^{III} atoms is virtually isotropic; the C−N distances for the cyanide ligands are similar, ranging from 1.149 to 1.176 Å. The crystallographically equivalent, terminal Co^{II}

dx.doi.org/10.1021/ic201534e | *Inorg. Chem.* 2011, 50, 12045−12052

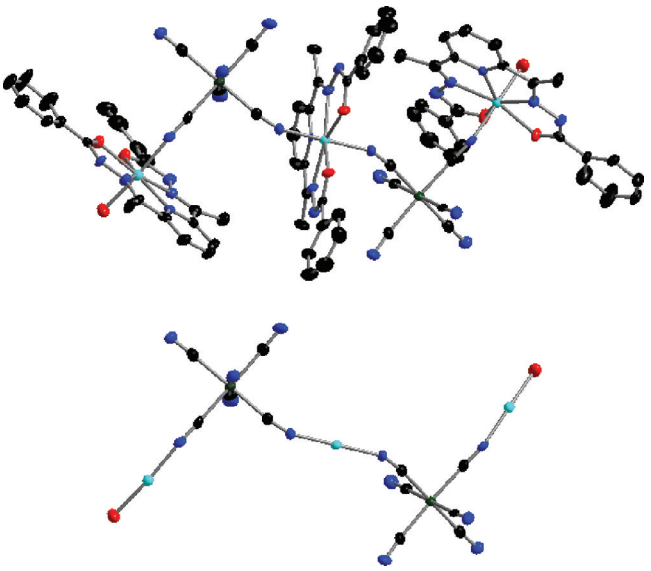

Figure 3. Structure of **4**. H atoms and solvent molecules are omitted for clarity (top), along with DABPH ligands (bottom). Color code: Co, cyan; Cr, green; C, black; N, blue; O, red. Thermal ellipsoids are shown at the 50% probability level.

moieties are bound to Cr^{III}-based cyano ligands cis to those bound to the central Co^{II}, resulting in an anti configuration for the zigzag pentametallic framework. The cyanide bridges are more linear than those at the central Co^{II} (a Co−N−C angle of 161.99°) and are slightly longer (a Co−N bond length of 2.093 Å). Again the pentagonal, equatorial planes are ligated by DABPH (ligand bite angles ranging from 70.32 to 76.69°), with water ligands occupying the terminal axial positions and numerous solvent water molecules in the crystal lattice. There is evidence of intramolecular $\pi-\pi$ interactions between the interwoven DABPH ligands of the terminal Co^{II} ions of adjacent clusters (separation ≈3.5 Å).

Similarly, the room temperature reaction of **1** with 1 equiv of $K_3[Fe(CN)_6]$ in $MeOH/H_2O$ yields crystalline **5** (Figure 4)

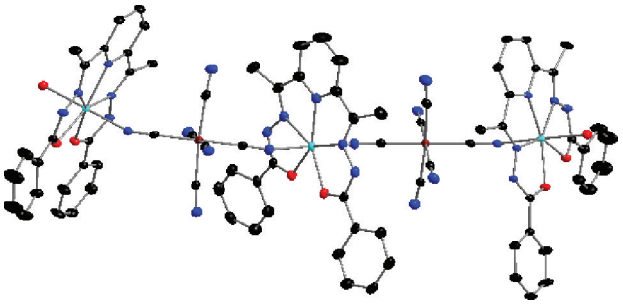

Figure 4. Structure of **5**. H atoms and solvent molecules are omitted for clarity. Color code: Co, cyan; Fe, brown; C, black; N, blue; O, red. Thermal ellipsoids are shown at the 50% probability level.

upon the slow evaporation of the reaction mixture. Elemental analysis of the precipitate corresponds to that expected from the crystal structure, and the IR spectra of the two materials are identical (showing both bridging and terminal CN groups at identical frequencies).

5 crystallizes in the monoclinic $C2/c$ space group and consists of a neutral, pentametallic cluster containing three $\{Co(DABPH)\}^{2+}$ units bridged to one another via two $\{Fe(CN)_6\}^{3-}$ moieties in an approximately linear fashion. Many structural features of **5** are similar to those of **4** (i.e., equatorial ligand bite angles in the range of 70.93−75.76° for the central Co^{II}, approximately isotropic environments around the Fe ions, terminal water molecules and solvent water molecules in the crystal lattice, and evidence of intramolecular $\pi-\pi$ interactions between the DABPH ligands of adjacent clusters), with the major difference being that the bridging iron-bound cyanides are trans to one another, inferring the overall linearity of the structure. Neither cyanide bridge is particularly straight in this case (Co−N−C angles are 155.94 and 153.05°). Bond-valence-sum analysis shows the oxidation states of the Co and Fe to be II+ and III+, respectively,[26] as is also required for charge balance.

The facile formation of these discrete $\{Co_3Cr_2\}$ and $\{Co_3Fe_2\}$ units can be attributed to their neutrality. There is no obvious capping ligand present in the reaction mixture so we postulate that the two components polymerize (facile substitution of labile water and nitrate ligands of {Co(DABPH}) by cyano N atoms from the anionic $[M(CN)_6]^{3-}$), with this neutral combination much less soluble than any of the charged permutations in the polar reaction media, thus crystallizing preferentially. The global structural difference (zigzag vs linear) may be due to the different ionic radii of Cr^{III} and Fe^{III}, with Fe^{III} being smaller with subsequently shorter distances between the metal ion and the cyano N atoms (≈3.09 Å compared to ≈3.21 Å for Cr^{III}) and steric hindrance subsequently preventing the {Co(DABPH)} fragments from linking cis to one another.

The IR spectra of **4** and **5** were recorded (see the Supporting Information). The fingerprint regions of the spectra are similar to that reported for **1**, with minor differences due to the minor conformational changes in the ligand. CN stretches are observed at 2127 cm^{-1} (**4**) and 2114 cm^{-1} (**5**), a frequency attributed to terminal rather than bridging cyanides in other reports;[21] however, close inspection of the peak for **4** reveals a shoulder toward higher frequency (as expected for bridging CN, where the stretching frequency is increased as a result of kinematic coupling),[27] suggesting that the bridging CN stretch is weaker and subsequently swamped by that of the terminal CN. For **5**, the full peak is observed for the bridging cyanides at 2138 cm^{-1}. It should also be noted that there is no evidence of $Cr^{III}-CN-Co^{II}$ to $Cr^{III}-NC-Co^{II}$ linkage isomerism (which would manifest as a CN stretch at ≈2100 cm^{-1}),[21] the occurrence of which can make crystallization of such systems difficult, and thus Co^{II} compounds of this type are much rarer than their Ni^{II} analogues.

Although the structure of **1** is published, magnetic data have not been reported for the complex. The measured molar magnetic susceptibilities (χ and χT) of **1** are plotted as a function of the temperature in Figure 5. The experiment was performed at 0.1 T (2−150 K) and 1.0 T (5−300 K) to assess any field dependence; none was observed in these ranges (as was the case for all five complexes investigated), and the 1.0 T data, for the larger temperature range, are plotted, overlaid with the 0.1 T data from 2 to 30 K (as is the case throughout). Also plotted is the measured magnetization as a function of the field. χT is ca. 2.26 emu K mol^{-1} at 300 K (larger than expected for the spin-only formula for a high-spin mononuclear Co^{II} complex, indicating a relevant orbital contribution) and remains constant down to 100 K, below which it collapses, reaching a value of 1.45 emu K mol^{-1} at 2 K, indicative of significant ZFS in the orbitally nondegenerate $S = {}^3/_2$ ground state. Similarly, at 2 K and 5.5 T, the observed magnetization value of 2.07 μ_B is

dx.doi.org/10.1021/ic201534e | Inorg. Chem. 2011, 50, 12045−12052

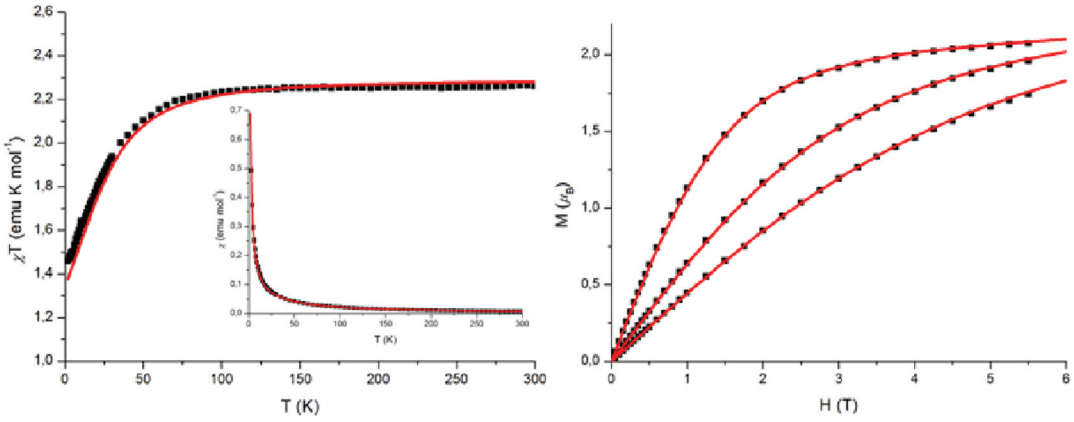

Figure 5. χT vs T (left) and χ vs T (inset) for **1** and M vs H (right) collected at 2, 4, and 6 K. Data were modeled using *MAGPACK* (solid line); see the text for parameters.

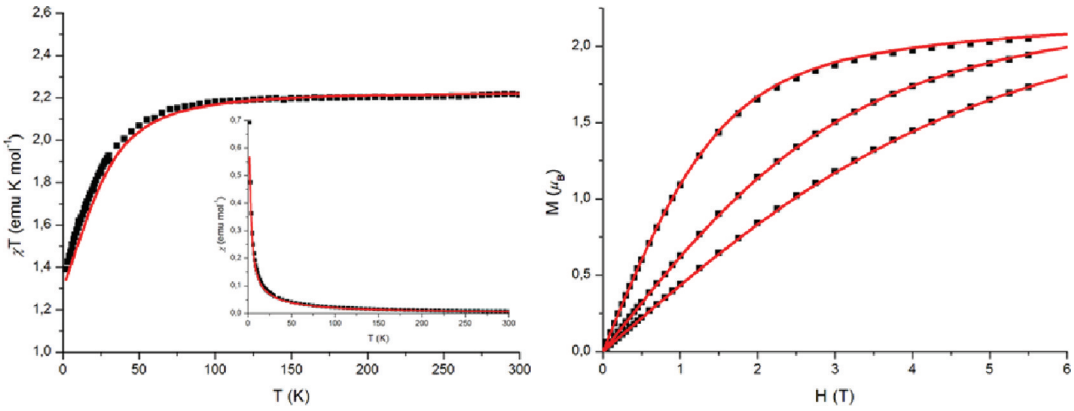

Figure 6. χT vs T (left) and χ vs T (inset) for **2** and M vs H (right) collected at 2, 4, and 6 K. Data were modeled using *MAGPACK* (solid line); see the text for parameters.

well below the theoretical saturation for an $S = {}^3/_2$ system (M_{sat} = 3.3 for g = 2.2), as expected when appreciable magnetic anisotropy is inherent. The data may be simulated with *MAGPACK* using Hamiltonian equation (1) and yielding the parameters g = 2.21, D = 32.0 cm^{-1}, and E = 0.3 cm^{-1} for the best fit.

$$H = g\mu_B \mathbf{S}\cdot\mathbf{B} + D\left[S_z^2 - \frac{1}{3}S(S+1)\right] + E[S_x^2 - S_y^2] \quad (1)$$

The fitting was performed simultaneously for the four experimental measurements (i.e., for the magnetization data at 2, 4, and 6 K and for the susceptibility data over the full temperature range), and to reduce the variable parameters during the fitting procedure, the g tensor was assumed to be isotropic. The g value was fixed according to the high-temperature χT value, with D and E then fit to the low-temperature regime and the magnetization data. The values obtained for g and D are consistent with those reported for other seven-coordinate Co^{II} complexes.[12] Initial attempts to model the data assumed purely axial ZFS (E = 0), but it was necessary to invoke the small rhombic term to ensure a good fit. In many cases, it is not possible to determine the sign of D from the magnetic data alone because there will be a range of values for D and E/D that yield equally adequate results; however, this is less likely when D is large, E/D is small, and the fit is performed for more than one temperature, affording us some certainty in the sign of D from these simulations.[28] Slow relaxation of magnetization has recently been observed for a monometallic first-row transition-metal complex (in which an Ising-type axial anisotropy was present);[29] however, given that in our case D is positive, it is unlikely that **1** will display slow relaxation of magnetization (as the $M_s = \pm{}^1/_2$ states of the $S = {}^3/_2$ ground state are stabilized). This anisotropic fragment could, however, be used to design larger SMMs provided the local ZFS tensors could be aligned to give rise to a molecular Ising-type anisotropy.[30] Additionally, the use of Co^{II} as a building block gives rise to the possibility of synthesizing molecules with noninteger ground states (Kramers doublets). In such cases, the $M_s = \pm x/2$ terms do not mix, independent of the magnitude of E, so quantum tunneling (one of the primary routes for magnetic relaxation in SMMs) may be eliminated.

2 (Figure 6) and **3** (Supporting Information) exhibit similar magnetic behavior, which can also be modeled using Hamiltonian equation (1), with the parameters g = 2.18, D = 30.0 cm^{-1}, and E = 0.3 cm^{-1} and g = 2.24, D = 30.0 cm^{-1}, and E = 0.3 cm^{-1}, respectively. One would perhaps expect the magnitude of the anisotropy to show greater dependence on the nature of the ligands belonging to the coordination sphere, as has already been reported.[31−33] This may be explained by considering the origin of the anisotropy, the interaction between the ground and first excited states of molecule. For the present case, the first excited state likely involves the electronic transition from the lowest-energy degenerate xz, yz

dx.doi.org/10.1021/ic201534e | Inorg. Chem. 2011, 50, 12045–12052

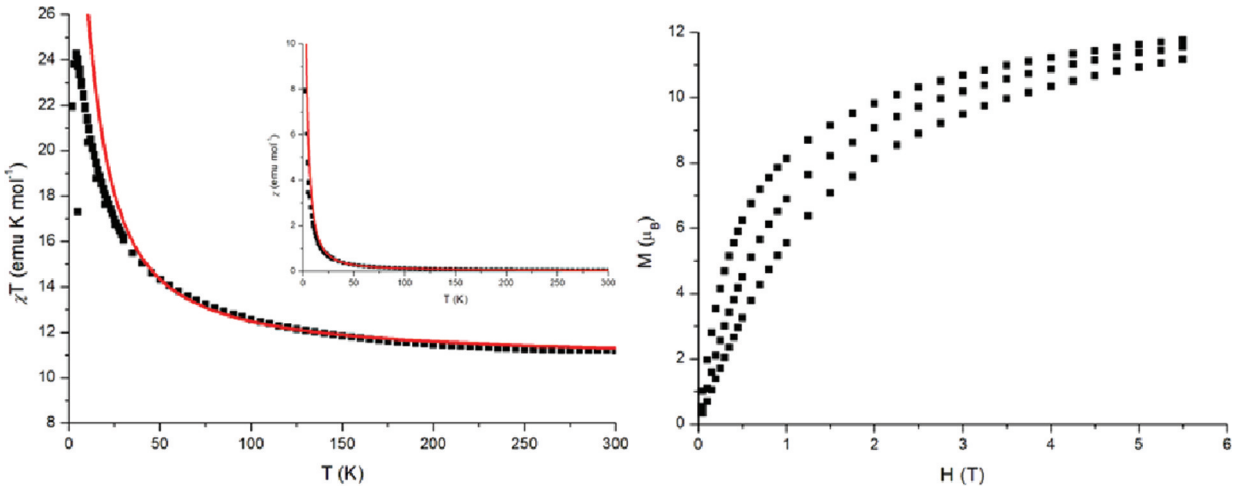

Figure 7. χT vs T (left) and χ vs T (inset) for **4** and M vs H (right) collected at 2, 4, and 6 K. Data were modeled using *MAGPACK* (solid lines); see the text for parameters.

orbitals to the xy, $x^2 - y^2$ set. Because the axial ligand primarily interacts with the z^2 orbital, it should have little effect on the energy of this transition, and thus on the anisotropy (to which it is inversely proportional). The minor difference could be due to the greater π character of the interaction with the heavy halides, which will affect the xz, yz set, although likely to a lesser extent, potentially changing the energy of the transition. Similar effects have been demonstrated in the case of five-coordinate Ni^{II} complexes.[34] Ab initio calculations are underway to rationalize the origin of the very large anisotropy found in the seven-coordinate Co^{II} complexes and the influence of the axial ligands on their magnitude.[35] At any rate, our experimental results show that the seven-coordinate Co^{II} moiety should possess a magnetic anisotropy largely unaffected by the nature of the axial ligands, making it a valuable building block for introducing significant local magnetic anisotropy into polynuclear species. Similar arguments may hold for other metals (e.g., Fe^{II}), which may exhibit Ising-type anisotropies that could again be inserted into larger systems; such work is currently underway.

The measured molar magnetic susceptibilities (χ and χT) of **4** are plotted as a function of the temperature in Figure 7. Also plotted is the measured magnetization as a function of the field. Upon cooling from room temperature, χT increases from 11.81 emu K mol^{-1} (slightly higher than expected for three uncoupled Co^{II} and two Cr^{III} ions, 10.56 emu K mol^{-1}, assuming $g_{Co} = 2.20$ and $g_{Cr} = 2.00$), reaches a maximum at 4 K (24.27 emu K mol^{-1}), and then decreases. This behavior implies ferromagnetic exchange between the metallic centers (as expected for pseudolinear Cr^{III}–CN–Co^{II} bridges),[36] although the maximum is well below that expected for an isolated $S = {}^{15}/_{2}$ ground state (≈38.5 emu K mol^{-1}). This is likely due to significant ZFS within the ground state and/or the proximity of low-lying excited states. Intermolecular antiferromagnetic exchange may also be present and would cause similar effects, and all of these factors would account for the collapse in χT below 4 K.

Assuming an idealized C_{5v} symmetry for the Co moieties (although the Co^{II} local geometries deviate slightly from the idealized one), the degeneracy of the 5d orbitals is lifted to three energy levels $e_1(xz,yz)$, $e_2(xy,x^2-y^2)$, and $a_1(z^2)$. The z^2 orbital is likely to remain the highest single occupied molecular orbital (SOMO), and the other two SOMOs, xy and $x^2 - y^2$, would contribute very little to the pseudolinear cyanide bridge along the Z axis of the Co^{II}. As such, a large ferromagnetic exchange coupling is expected because of interaction between orthogonal orbitals on the Co (z^2) and Cr (xz and yz). However, because the Co–N–C angles are smaller than 180°, the strict orthogonality criteria are not fulfilled and an antiferromagnetic contribution to the interaction will be present, which weakens the overall ferromagnetic exchange coupling.

A full simulation of the data using *MAGPACK* was impractical given the likelihood of overparametrization and the incapacity of the program to model relative anisotropic vectors (which will clearly play a defining role in determining the observed magnetic behavior in this case, close to the weak exchange limit); however, a reasonable fit of the susceptibility data can be obtained to 30 K using *ISOTROPIC MAGPACK* (neglecting local anisotropies), providing some insight into the strength of the intramolecular exchange interactions. An adequate fit was obtained with a simplistic one J model (assuming each Cr^{III}–CN–Co^{II} bridge to be equal and no other exchange interactions to be in operation), using Hamiltonian equation (2), yielding parameters $g_{average} = 2.14$ and $J = 2.7$ cm^{-1}.

$$H = -2J(S_1 \cdot S_2 + S_2 \cdot S_3 + S_3 \cdot S_4 + S_4 \cdot S_5) \quad (2)$$

It is unlikely that the two sets of cyanide bridges actually present the same magnitude of exchange (given the different Co–N–C angles), but the one J model provides an adequate fit (in agreement with other reported Cr–CN–Co exchanges)[19] given the limited data that is modeled. Furthermore, this value can at best be referred to as an "effective" exchange because the fit is to the net result of the two competitive factors affecting the magnitude of χT at a given temperature: (1) the ferromagnetic exchange between metal ions and (2) the significant local anisotropy, observed to have a large effect up to 100 K in the monomers; thus, the absolute value of J is likely somewhat larger. This set of parameters obviously did not provide a good fit for the magnetization versus field data, the low-temperature, high-field experimental regime that is dominated by the effects of local, and subsequently molecular, anisotropy. The magnetization value at 2 K and 5.5 T of 11.8 μ_B is below that expected for a $S = {}^{15}/_{2}$ ground state (≈16 μ_B assuming $g = 2.14$) and has not reached a plateau, implying an

dx.doi.org/10.1021/ic201534e | *Inorg. Chem.* 2011, 50, 12045–12052

anisotropic and/or poorly isolated ground state. We initially considered modeling the data with a giant spin, $S = {}^{15}/_{2}$; however, this was deemed inappropriate. Even using eigenvalues extracted from the isotropic model, considering only the exchange, the $S = {}^{15}/_{2}$ ground state is separated from the first $S = {}^{13}/_{2}$ excited state by only 3.1 cm^{-1}, and the introduction of significant positive local anisotropies at the Co^{II} sites will further reduce this separation. Thus, it is highly unlikely that there is one state uniquely populated even in the low-temperature, high-field regime. Future work will include a more thorough investigation of this situation by our theoretical collaborators.

Given the large anisotropic ground state of **4**, preliminary alternating-current measurements were performed; however, because we believe the ZFS to be positive, it was an unlikely candidate for SMM behavior, and the effect was not observed. There was a slight increase in the out-of-phase susceptibility component toward 1.8 K; however, no maximum was observed, and furthermore there was a 2 order difference in magnitude between the in-phase and out-of-phase components.

A plot of χT as a function of the temperature for **5** is shown in Figure 8. Also plotted is the measured magnetization as a function of the field. Upon cooling from room temperature, χT gradually increases from 7.95 emu K mol^{-1} (slightly higher than expected for three uncoupled Co^{II} and two Fe^{III} ions, 7.56 emu K mol^{-1}, assuming $g_{Co} = 2.20$ and $g_{Fe} = 2.00$), reaches a maximum at approximately 85 K (8.23 emu K mol^{-1}), and then decreases to a minimum at 15 K (7.68 emu K mol^{-1}) before finally increasing toward its second maximum at 4 K (8.09 emu K mol^{-1}). This behavior may be rationalized as follows. The increase between 300 and 85 K is the net result of the opposing effects of ferromagnetic exchange between metal centers and large local anisotropy at the metal centers. The "effective" exchange appears weaker than that in **4**, which may be due to weaker absolute exchange between metal ions, due to differences in the bridging angles for the cyanides, or it may be due to the greater combined effects of the local anisotropies of the Co^{II} ions due to the colinear arrangement of the magnetic axes compared to the orthogonal arrangement in **4**. The decrease between 85 and 15 K reflects the greater effect of the local anisotropies on χT at temperatures below 100 K, as observed for the monomers **1**–**3**. At very low temperatures (below 15 K), the lowest-energy Kramers doublet (effective spin $S' = {}^{1}/_{2}$) may be uniquely populated and the increase in χT is assumed to be due to the ferromagnetic exchange between the effective $S' = {}^{1}/_{2}$ Co^{II} ions and the $S = {}^{1}/_{2}$ Fe^{III} ions, which becomes dominant at low temperature. Similar behavior has been reported for ferromagnetically coupled Co^{II} macrocycles, albeit concerning octahedral Co^{II} species.[37]

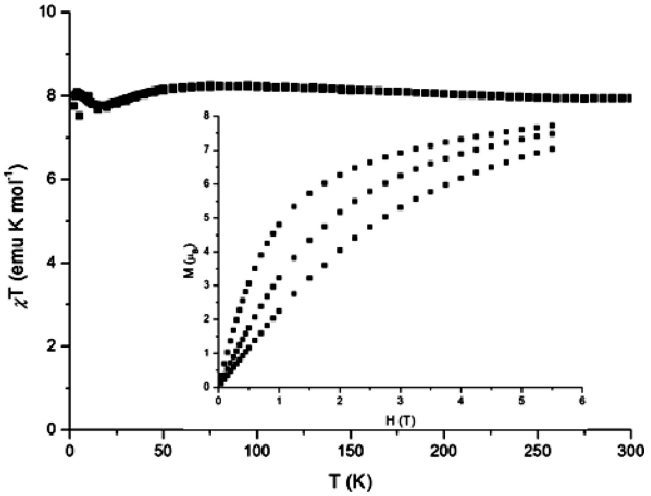

Figure 8. χT vs T for **5** and M vs H (inset) collected at 2, 4, and 6 K.

The magnetization value at 2 K and 5.5 T (7.72 μ_B) is below that expected for a well-isolated $S = {}^{11}/_{2}$ ground state and is indicative of substantial magnetic anisotropy. Given the limitations in our attempts to model the data for **4** and the range of parameters that could be governing the behavior of our relatively limited data set, attempts were not made to model the data at this time. The very different behaviors observed for **4** and **5** likely due to the different arrangements of the local magnetic axes demand further investigation; attempts to synthesize the $[\{Co(DABPH)\}_3\{Co^{III}(CN)_6\}_2(H_2O)_2]$ cluster are underway because the diamagnetic bridging Co^{III} moieties would negate the effects of magnetic exchange and may shed light on the relationship between the local and molecular anisotropies and the local geometry.

CONCLUSION

In summary, seven-coordinate $[Co(DABPH)X_2]$ is a very anisotropic $S = {}^{3}/_{2}$ molecular fragment, with two labile axial ligands and the local anisotropy largely independent of the character of those ligands. This can be incorporated into larger clusters and may be used to promote large molecular anisotropies. A thorough investigation of other less common geometries among first-row transition metals (i.e., five- or seven-coordinate) and their use as building blocks is also underway, particularly Ni^{II} and Fe^{II}, which should possess huge, and not necessarily positive, local anisotropies due to near-degeneracy effects, affording us a greater range of tools in the search for greater anisotropy in high-spin clusters.

ASSOCIATED CONTENT

Supporting Information

IR spectra of compounds **4** and **5** and plots of magnetic susceptibility versus temperature and magnetization versus field for compound **3** including *MAGPACK* simulation. This material is available free of charge via the Internet at http://pubs.acs.org. CCDC 835139, 835140, and 835141 contain the supplementary crystallographic data for this paper. These data can be obtained free of charge from the Cambridge Crystallographic Data Centre via www.ccdc.cam.ac.uk/data_request/cif.

AUTHOR INFORMATION

Corresponding Author

*E-mail: luke.batchelor@u-psud.fr (L.J.B.), talal.mallah@u-psud.fr (T.M.). Tel: (+33) (0)1 69 15 47 49. Fax: (+33) (0) 1 69 15 47 54.

REFERENCES

(1) Sessoli, R.; Tsai, H. L.; Schake, A. R.; Wang, S.; Vincent, J. B.; Folting, K.; Gatteschi, D.; Christou, G.; Hendrickson, D. N. *J. Am. Chem. Soc.* **1993**, *115*, 1804.

(2) Aromí, G.; Brechin, E. *Struct. Bonding (Berlin)* **2006**, *122*, 1.

(3) Troiani, F.; Ghirri, A.; Affronte, M.; Carretta, S.; Santini, P.; Amoretti, G.; Piligkos, S.; Timco, G.; Winpenny, R. E. P. *Phys. Rev. Lett.* **2005**, *94*, 207208.

(4) Larionova, J.; Gross, M.; Pilkington, M.; Andres, H.; Stoeckli-Evans, H.; Güdel, H. U.; Decurtins, S. *Angew. Chem., Int. Ed.* **2000**, *39*, 1605.
(5) Murugesu, M.; Habrych, M.; Wernsdorfer, W.; Abboud, K. A.; Christou, G. *J. Am. Chem. Soc.* **2004**, *126*, 4766.
(6) Barra, A.-L.; Brunel, L.-C.; Gatteschi, D.; Pardi, L.; Sessoli, R. *Acc. Chem. Res.* **1998**, *31*, 460.
(7) Murrie, M. *Chem. Soc. Rev.* **2011**, *39*, 1986.
(8) Boca, R. *Coord. Chem. Rev.* **2004**, *248*, 757.
(9) En-Che, Y.; David, N. H.; Wolfgang, W.; Motohiro, N.; Lev, N. Z.; Roger, D. S.; Arnold, L. R.; Marisol, L.-G.; George, C. *J. Appl. Phys.* **2002**, *91*, 7382.
(10) Langley, S. J.; Helliwell, M.; Sessoli, R.; Rosa, P.; Wernsdorfer, W.; Winpenny, R. E. P. *Chem. Commun.* **2005**, 5029.
(11) Yoshihara, D.; Karasawa, S.; Koga, N. *J. Am. Chem. Soc.* **2008**, *130*, 10460.
(12) Platas-Iglesias, C.; Vaiana, L.; Esteban-Gomez, D.; Avecilla, F.; Real, J. A.; de Blas, A.; Rodriguez-Blas, T. *Inorg. Chem.* **2005**, *44*, 9704.
(13) Mathieu, F.; Weiss, R. *J. Chem. Soc., Chem. Commun.* **1973**, 816a.
(14) Gou, S.; You, X.; Yu, K.; Lu, J. *Inorg. Chem.* **1993**, *32*, 1883.
(15) Fewings, K. R.; Junk, P. C.; Georganopoulou, D.; Prince, P. D.; Steed, J. W. *Polyhedron* **2001**, *20*, 643.
(16) Andelkovic, K.; Ivanovic, I.; Prelesnik, B. V.; Leovac, V. M.; Poleti, D. *Polyhedron* **1996**, *15*, 4361.
(17) Barrios, L. A.; Aguila, D.; Roubeau, O.; Murray, K. S.; Aromi, G. *Aust. J. Chem.* **2009**, *62*, 1130.
(18) Rajput, L.; Biradha, K. *Cryst. Growth Des.* **2007**, *7*, 2376.
(19) Zhang, Y.-Z.; Sato, O. *Inorg. Chem.* **2009**, *49*, 1271.
(20) Beltran, L. M. C.; Long, J. R. *Acc. Chem. Res.* **2005**, *38*, 325.
(21) Shatruk, M.; Chambers, K. E.; Prosvirin, A. V.; Dunbar, K. R. *Inorg. Chem.* **2007**, *46*, 5155.
(22) Giordano, T. J.; Palenik, G. J.; Palenik, R. C.; Sullivan, D. A. *Inorg. Chem.* **1979**, *18*, 2445.
(23) Borrás-Almenar, J. J.; Clemente-Juan, J. M.; Coronado, E.; Tsukerblat, B. S. *J. Comput. Chem.* **2001**, *22*, 985.
(24) Sheldrick, G. M. *SHELX-97*; Universitat Gottingen: Gottingen, Germany, 1997.
(25) Shiga, T.; Okawa, H.; Kitagawa, S.; Ohba, M. *J. Am. Chem. Soc.* **2006**, *128*, 16426.
(26) Brese, N. E.; O'Keeffe, M. *Acta Crystallogr.* **1991**, *B47*, 192.
(27) Bignozzi, C. A.; Argazzi, R.; Schoonover, J. R.; Gordon, K. C.; Dyer, R. B.; Scandola, F. *Inorg. Chem.* **1992**, *31*, 5260.
(28) Rogez, G. Ph.D. Thesis, Université Paris Sud XI, Orsay, France, 2002.
(29) Freedman, D. E.; Harman, W. H.; Harris, T. D.; Long, G. J.; Chang, C. J.; Long, J. R. *J. Am. Chem. Soc.* **2011**, *132*, 1224.
(30) Rebilly, J.-N.; Mallah, T. *Struct. Bonding (Berlin)* **2006**, *122*, 103.
(31) Desrochers, P. J.; Telser, J.; Zvyagin, S. A.; Ozarowski, A.; Krzystek, J.; Vicic, D. A. *Inorg. Chem.* **2006**, *45*, 8930.
(32) Duboc, C.; Phoeung, T.; Zein, S.; Pecaut, J.; Collomb, M. N.; Neese, F. *Inorg. Chem.* **2007**, *46*, 4905.
(33) Long, J. R.; Karunadasa, H. I.; Arquero, K. D.; Berben, L. A. *Inorg. Chem.* **2010**, *49*, 4738.
(34) Rebilly, J.-N.; Charron, G.; Rivière, E.; Guillot, R.; Barra, A.-L.; Serrano, M.-D.; van Slageren, J.; Mallah, T. *Chem.—Eur. J.* **2008**, *14*, 1169.
(35) Ruamps, R.; Maurice, R.; Guihery, N.; Gogoi, N., ; Sutter, J.-P.; Batchelor, L. J.; Mallah, T. Manuscript in preparation. 2011.
(36) Mallah, T.; Auberger, C.; Verdaguer, M.; Veillet, P. *J. Chem. Soc., Chem. Commun.* **1995**, 61.
(37) Moragues-Canovas, M.; Talbot-Eeckelaers, C. E.; Catala, L.; Lloret, F.; Wernsdorfer, W.; Brechin, E. K.; Mallah, T. *Inorg. Chem.* **2006**, *45*, 7038.